ELSEVIER

The mechanism of ethylene polymerization by nickel salicylaldiminato catalysts – Agostic interactions and their kinetic isotope effects

Alexander Zeller, Thomas Strassner *

Technische Universitaet Dresden, Physikalische Organische Chemie, Mommsenstr. 13, D-01062 Dresden, Germany

Abstract

The ethylene polymerization reaction of a neutral nickel catalyst was studied by DFT calculations at the Becke3LYP/6-31G(d) level of theory. As in related cases a β-agostic bond stabilizes the nickel alkyl ground states. Transition states for the insertion of the olefin show a distinct α-agostic interaction, which has not been observed for late metal polymerization catalysts before. An ethylene–alkyl complex was identified as the resting state of the reaction. The overall barrier height of the reaction amounts to 17.54 kcal/mol, which slightly increases to 17.60 kcal/mol for the polymerization of deuterated ethylene. Therefore, a small positive kinetic isotope effect ($k_H/k_D = 1.09$) can be calculated, which is caused by the α-agostic interaction in the transition state. A comparison to other late metal based polymerization systems reveals that the ethylene coordination step of highly active catalysts is significantly lower in energy compared to catalysts which are only moderately active.
© 2006 Elsevier B.V. All rights reserved.

1. Introduction

Kinetic isotope effects (KIE) are a great tool to get insight into reaction mechanisms, since changes in the mechanism can lead to major differences in the KIE of the overall reaction [1,2]. Especially in the field of olefin polymerization catalysis, kinetic isotope effects reveal the presence or absence of agostic interactions in intermediates of the catalytic cycle. α-Agostic interactions in the transition state of the olefin insertion were discussed for metallocene catalysts, leading to a KIE in the range of 1.2–1.3 [3–7]. A theoretical study confirmed that this interaction lowers the barrier for the olefin insertion by stabilization of the transition state and contributes to the stereospecificity of the reaction [8]. Up to now α-agostic interactions of this type have only been observed for early transition metal

catalysts, where their existence could be confirmed by a large number of theoretical studies [9–14]. For all single-site catalysts it is known, that polymerization ground states (usually low-coordinate metal–alkyl complexes) can exhibit different agostic interactions, most importantly α-, β- and γ-interactions [9,15,16]. In most cases the β-agostic geometry corresponds to the most stable form. This is also true for late transition metal catalysts [17,18] as shown by several theoretical studies [19–25]. For a Co(III)-catalyst the β-agostic complex is equivalent to the resting state of the polymerization reaction which leads to a pronounced inverse kinetic isotope effect [26,27].

Recently, the Grubbs group introduced a new class of neutral nickel olefin polymerization catalysts based on salicylaldiminato ligands (Fig. 1, Structure **I**) [28,29]. They are particularly attractive, as they do not require activation by MAO and tolerate functional groups in polar monomers. Later, the catalyst was modified by Brookhart et al. by incorporating five-membered chelate ligands instead of

---

* Corresponding author. Fax: +49 351 463 39679.
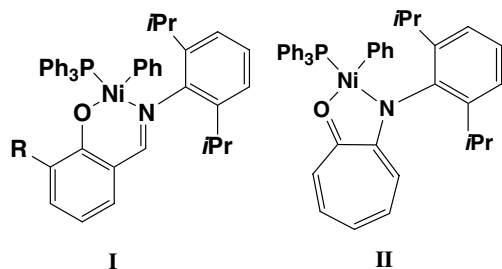 *E-mail address:* thomas.strassner@chemie.tu-dresden.de (T. Strassner).

Fig. 1. Highly active neutral nickel ethylene polymerization catalysts.

the initially used six-membered system (Fig. 1, Structure **II**) [30–32]. Whereas for the later class a full quantum-mechanical DFT study on the complete ethylene polymerization cycle was presented [33], related reports on the Grubbs system rely on smaller model systems or a QM/MM-approach [34–37]. Moreover, energetic discussions are based on electronic energies. Additionally, detailed calculations on the polymerization with higher olefins or functionalized monomers have been performed [35,36,38,39].

Herein, we want to report DFT calculations for the catalyst system **I**. One entire polymerization cycle was investigated including a free energy analysis. This is crucial for identifying the resting state and the rate-determining transition state of the reaction. To obtain information about the influence of agostic interactions, which could be identified in several intermediates, the results were used for a theoretical prediction of the kinetic isotope effect of the

polymerization. Furthermore, a comparison to other late metal based catalysts may lead to valuable insight into structure–activity relationships.

2. Results and discussion

2.1. Mechanism of the polymerization reaction

A polymerization cycle of the active species, derived from catalyst **I** (R = H) by dissociation of the weakly coordinating ligand, was optimized according to the Cossee–Arlman mechanism [40–42] on the Becke3LYP/6-31G(d) level of theory without simplifications on the ligand (Scheme 1). Three-dimensional representations are depicted in Fig. 2; geometric parameters can be found in Table 1. To model the influence of the polymer chain properly we chose the propyl complexes 1_O and 1_N as starting points of the cycle. As reported previously [34], due to the asymmetry of the ligand two alternative reaction pathways have to be considered. They either start from an alkyl substituent coordinated *trans* to the oxygen atom (Pathway A) or *trans* to the nitrogen atom of the ligand (Pathway B). In the course of the ethene insertion the alkyl substituent changes it position, i.e. if it is bound in *trans* position to the oxygen atom the longer alkyl chain appears in *trans* position to the nitrogen atom (and vice versa). We did not look at transition states for the coordination of ethene as they are known to be energetically well below the insertion transition states [27,43].
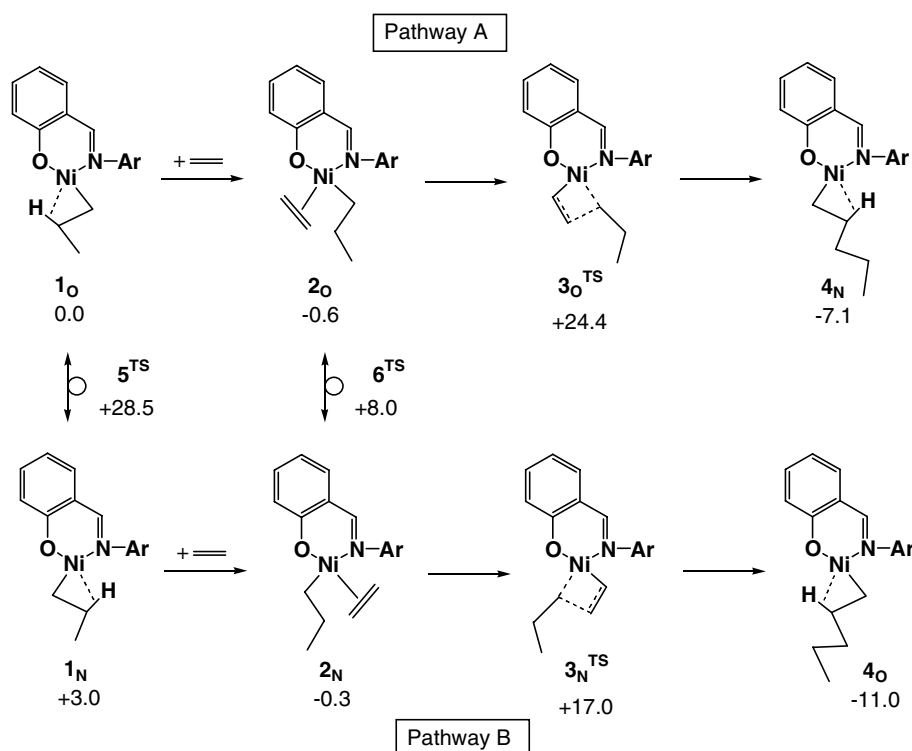
Scheme 1. Important intermediates in the polymerization cycle of catalyst **I** (structures with an alkyl chain in *trans*-position to N or O are denoted by **N** and **O**, respectively).
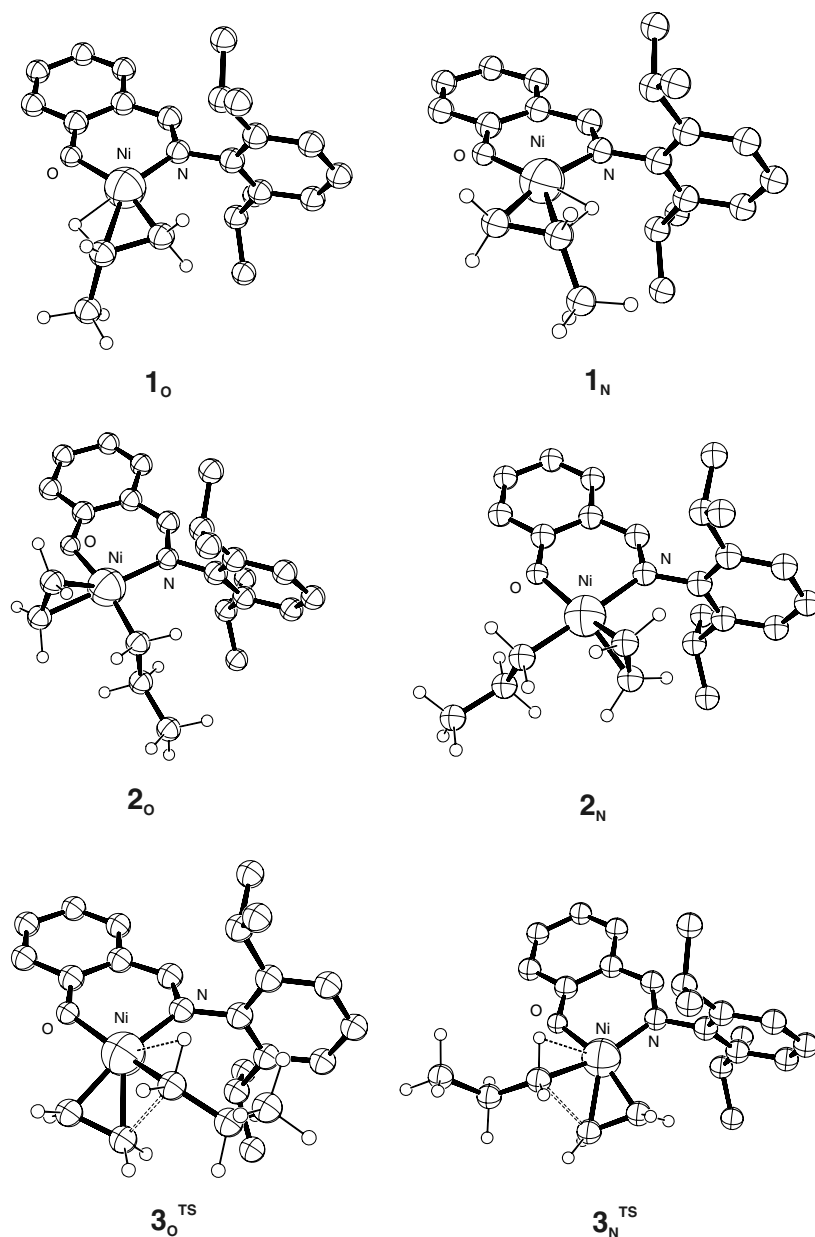
Fig. 2. Three-dimensional representations of **1**–**3** (hydrogen atoms on the ligand have been omitted for clarity).

As in related threefold coordinated nickel alkyl structures the starting ground state structures $\mathbf{1_O/4_O}$ and $\mathbf{1_N/4_N}$ are stabilized by an β-agostic interaction. This interaction is somewhat stronger for the oxygen atom situated in the *trans*-position in $\mathbf{1_O/4_O}$ (obvious from the shorter $Ni–H_{\beta\text{-agost.}}$ and longer $C_\beta–H_{\beta\text{-agost.}}$-distance). Accordingly, the complex $\mathbf{1_N}$ is 3.0 kcal/mol higher in energy relative to $\mathbf{1_O}$ (3.9 kcal/mol for $\mathbf{4_N}$ and $\mathbf{4_O}$). The reason is, that in $\mathbf{1_N}$ and $\mathbf{4_N}$ the alkyl chain is forced in a sterically unfavorable position close to the aryl substituent, which is not the case for $\mathbf{1_O}$ and $\mathbf{4_O}$. Coordination of ethylene generates the alkyl–ethylene structures $\mathbf{2_O}$ and $\mathbf{2_N}$, respectively. They both show structural displacements due to steric constraints induced by the bulky aryl residue. In $\mathbf{2_O}$ this leads to a distortion around the nickel center, whereas in $\mathbf{2_N}$ the

diisopropylphenyl substituent is forced in an almost upright position with respect to the metal–ligand plane. Despite their crowded arrangement, structures $\mathbf{2_O}$ and $\mathbf{2_N}$ are slightly lower in energy compared to the β-agostic precursors. In the following transition states ($\mathbf{3_O^{TS}}$ and $\mathbf{3_N^{TS}}$) the ethylene ligand rotates into the metal–ligand plane. In this manner steric constraints should be reduced, but in fact this is only possible for the sequence $\mathbf{2_N/3_N^{TS}}$. Within $\mathbf{3_O^{TS}}$ strong steric interactions remain between the propyl and the aryl group. This seems to be the reason why $\mathbf{3_N^{TS}}$ is much more energetically favorable compared to $\mathbf{3_O^{TS}}$ ($\Delta\Delta G = 7.4$ kcal/mol) [44]. This suggests that the polymerization reaction proceeds almost exclusively via transition state $\mathbf{3_N^{TS}}$. The barrier height for $\mathbf{3_N^{TS}}$ (17.6 kcal/mol relative to ground state $\mathbf{2_O}$) compares very well with previously

Table 1
Selected bond distances of **1**–**3** in Å

	$1_O/4_O$	$1_N/4_N$
Ni—O	1.85	1.81
Ni—N	1.83	1.91
Ni—C_α	1.86	1.87
Ni—C_β	2.15	2.11
Ni—$H_{\beta\text{-agost.}}$	1.69	1.63
C_α—C_β	1.50	1.49
C_β—$H_{\beta\text{-agost.}}$	1.16	1.18

	2_O	2_N	3_O^{TS}	3_N^{TS}
Ni—O	1.90	1.86	1.85	1.89
Ni—N	1.97	2.03	1.99	1.90
Ni—C_α	1.92	1.93	2.08	2.05
Ni—$H_{\alpha\text{-agost.}}$	–	–	2.09	2.05
Ni—C_β	2.79	2.84	3.37	3.19
C_α—$H_{\alpha\text{-agost.}}$	–	–	1.10	1.10
C_α—C_β	1.53	1.53	1.53	1.52
Ni—C_{Ethen}	2.00/2.04	1.98/2.00	1.91/2.07	1.91/2.03
C_{Ethen}—C_{Ethen}	1.39	1.39	1.43	1.44
C_α—C_{Ethen}	–	–	2.01	2.05

Table 2
Selected bond distances of **5^{TS}** and **6^{TS}** in Å

	5^{TS}		6^{TS}
Ni—O	1.89	Ni—O	1.90
Ni—N	1.94	Ni—N	2.02
Ni—C_α	1.84	Ni—C_α	1.91
Ni—C_β	2.18	Ni—C_β	2.86
Ni—$H_{\beta\text{-agost.}}$	1.72	C_α—C_β	1.52
C_α—C_β	1.50	Ni—C_{Ethen}	1.93/1.95
C_β—$H_{\beta\text{-agost.}}$	1.16	C_{Ethen}—C_{Ethen}	1.42

determined experimental values of 16–17 kcal/mol [43] for ethylene insertion in the anilinotropone system **II** [44]. An interesting feature of both transition states for olefin insertion is a distinct α-agostic interaction of the alkyl chain with the nickel center (Ni—$C_{\alpha\text{-agost.}}$ = 2.08/2.05 Å; Ni—$H_{\alpha\text{-agost.}}$ = 2.09/2.05 Å). To the best of our knowledge, this has not been reported for late transition metal catalysts before. In DFT studies of Brookhart's nickel diimine systems [19,45] significantly longer Ni—$H_{\alpha\text{-agost.}}$ distances of about 2.3 Å were found. The same is true for a recently investigated, tetrahedral Co(III)-catalyst [27].

As reported previously, due to the large energy difference between both insertion transition states a change of the relative position of the alkyl chain during the polymerization cycle is likely. This exchange can occur between the β-agostic ground states **1$_O$** and **1$_N$** or between the alkyl–ethylene structures **2$_O$** and **2$_N$**. Both transition states (**5^{TS}** and **6^{TS}**) could be optimized (three-dimensional representations are depicted in Fig. 3; geometric parameters can be found in Table 2).

In **5^{TS}** the vertically arranged propyl substituent remains in a β-agostic geometry, i.e. the Ni—$C_{\beta\text{-agost.}}$ and Ni—$H_{\beta\text{-agost.}}$ contacts are almost as close as in **1$_O$** and **1$_N$**. In the alkyl–ethylene transition state **6^{TS}** a slightly longer C—C bond distance for ethene (compared to the ground states **2$_O$** and **2$_N$**) is observed, indicating a stronger interaction of the π-orbitals with the metal. Interestingly, the olefin ligand remains in the metal–ligand plane, whereas the alkyl group is bent towards an octahedral position of the nickel center. If one compares the energy of the transition states **5^{TS}** and **6^{TS}** (+28.5 and +8.0 kcal/mol, respectively), it is obvious that the change of the coordination sites has to proceed via the latter [44].

2.2. Prediction of the kinetic isotope effect

For a prediction of the KIE the course of the reaction on the free energy surface is important, since the KIE is determined by the barrier height between the resting state and the rate-determining transition state. From our calculations, the ethylene–alkyl complexes **2$_O$** and **2$_N$** are the lowest ground states in the gas phase. This assumption is supported by experimental studies of the related catalyst **II**, which revealed that under actual polymerization conditions a nickel alkyl–ethylene complex is the resting state of the reaction [43,46]. For the KIE calculation **2$_O$** was used since it is 0.3 kcal/mol lower in energy than **2$_N$** (and it is predicted that the lowest energy pathway proceeds via both ground states). The rate-determining transition state on the lowest energy pathway corresponds to **3$_N^{TS}$**. Based
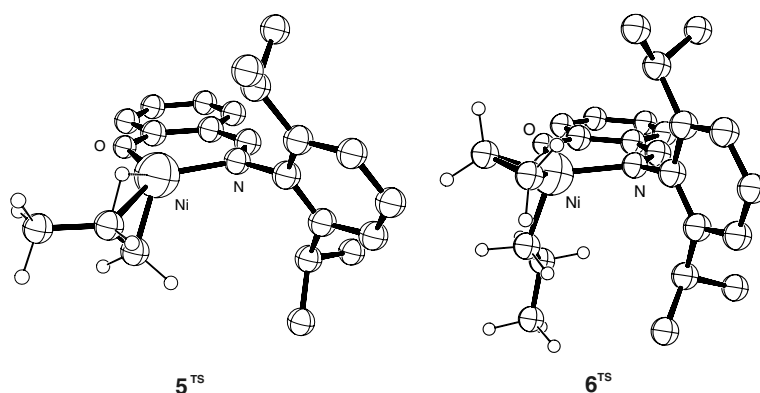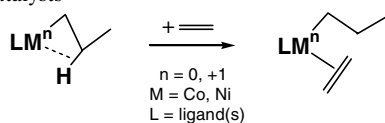

Fig. 3. Three-dimensional representations of isomerization transition states **5^{TS}** to **6^{TS}** (hydrogen atoms on the ligand have been omitted for clarity).

Table 3
Ethylene complexation energy of various late metal catalysts

Catalyst (ligand system)	Activity	$\Delta E_{\text{Complexation}}$ (in kcal/mol)	$\Delta G_{\text{Complexation}}$ (in kcal/mol)	Literature
Co(III) (Cp*; P(OMe)$_3$)	Moderate	−4.8[a]	+10.1[a]	[27]
Warren (β-diketiminate)	Moderate	−5.0[a]	+13.2[a]	[25]
Grubbs (salicylaldiminato)	High	−15.9/−15.6[a]	−0.3/−0.6[a]	This work
Brookhart (diimine)	High	−13.7[b]	+1.9[b]	[62]
Brookhart (anilinotropone)	High	−18.8/−20.5[b]	∼−6 to −8[b,c]	[33]

[a] Becke3LYP/6-31G*.
[b] ADF calculations.
[c] A general value of +12.5 kcal/mol for $-T\Delta S$ was given.

on these assumptions the activation barrier of the polymerization amounts to $\Delta G_H = 17.54$ kcal/mol. If ethylene is replaced by ethylene-d_4 the barrier slightly increases to $\Delta G_D = 17.60$ kcal/mol. This difference leads to a small positive KIE of $k_H/k_D = 1.09$ for the polymerization reaction [44]. This secondary isotope effect is caused by the α-agostic C—H bond in the transition state, which remains unbound in the ground state. Therefore, the vibrational frequency of the C—H(D) bond in the transition state is lower relative to the ground state. This results in a larger zero point energy difference in the ground state relative to the transition state, which leads to the positive KIE [26]. Calculations of the KIE were repeated for the case of a β-agostic resting state. For $\mathbf{1_O}$ as the ground state, an inverse kinetic isotope effect of 0.58 is predicted ($\Delta G_H = 16.95$ and $\Delta G_D = 16.63$ kcal/mol). This means, that the strength of the β-agostic bond in $\mathbf{1_{O/N}}$ should exceed the strength of the α-agostic interaction in the transition state. From these results experiments comparing activities in the polymerization of ethylene and ethylene-d_4 should provide detailed insight about the lowest-energy ground state and the reaction mechanism of this catalyst. From our calculations the salicylaldimine catalyst is the first system containing a late transition metal for which a KIE of larger than 1 is possible.

Herein, we also want to report theoretically derived KIEs for the polymerization of ^{13}C-enriched ethylene. Our calculations show a predicted $k(^{12}C)/k(^{13}C) = 1.041$ for the case of an alkyl–ethylene resting state in the polymerization catalyzed by $\mathbf{I}$. For a β-agostic resting state the corresponding KIE would be 1.043, which means that an experimental measurement of the $^{12}C/^{13}C$-KIE could hardly discriminate between both mechanisms. Therefore in this case it is not possible to use the elegant technique for the measurement of $^{12}C/^{13}C$- (and $^1H/^2H$-) KIEs, which was recently introduced by Singleton and coworkers [47–49]. It provides the possibility to detect position-specific KIEs at natural abundance. This technique has for example been used to investigate the mechanism of the 1-hexene polymerization by an *ansa*-metallocene catalyst [50].

3. Comparison to other late metal polymerization catalysts

Generally, for ethylene polymerization catalysts the migratory insertion is the rate-determining step in the reaction, but the catalyst behavior significantly changes throughout the periodic table. For early transition metals a first-order or higher dependence on olefin concentration is observed [9,15,51]. In contrast, NMR studies of the nickel diimine catalysts by Brookhart et al. revealed that the chain growth is zero-order in ethylene, which is evidence for an alkyl–ethylene resting state [52,53]. This was also experimentally observed for other highly active cationic nickel systems [54]. Earlier calculations, especially on small model systems, had problems to describe the energetics of the olefin coordination properly [9,27]. For the Becke3LYP functional at least a 6-31G(d) basis set is necessary for an accurate description of the olefin bond.

From the data we collected we propose that the potential activity of a catalyst might be derived from the corresponding olefin complexation energy of the β-agostic structure. Results are shown in Table 3, where known activities of various cobalt and nickel catalysts are summarized, together with literature values of the complexation energy of ethylene.

The height of the insertion barrier is decisive for the activity of a polymerization catalyst. Results from many DFT studies suggest that this barrier is comparable for most first-row late metal polymerization systems. From the data in Table 3 it is evident, that the olefin complexation energy is more important for the observed polymerization activity. Thus, screening for further promising catalyst candidates can be supported by a determination of the free energy difference of this polymerization step, which should be well below −10 kcal/mol for ΔE and around or below 0 kcal/mol for ΔG on the Becke3LYP/6-31G(d) level of theory.

4. Conclusion

The ethylene polymerization catalyzed by a neutral salicyldiminato nickel catalyst was studied by double-ζ DFT

calculations without simplifications of the ligand system. This allows the calculation of thermodynamic data for this particularly interesting polymerization catalyst. It was found, that the barrier of ethylene insertion on the lowest-energy pathway amounts to 17.3 kcal/mol, which agrees very well with experimental results of related nickel systems. Furthermore, an analysis of the catalytic cycle including entropic contributions allows an identification of the resting state of the reaction, which corresponds to the alkyl–ethylene complex. In the insertion transition state an α-agostic interaction of the alkyl chain with the metal center was observed. Accordingly, a positive kinetic isotope effect of 1.09 was calculated for the polymerization of C_2H_4 vs. C_2D_4. This was previously only found for early transition metal catalysts, which showed KIEs in the range of 1.2–1.3.

We identified a possible correlation between the energetics of the olefin coordination, the activation barrier and the activity of the late transition metal catalyst systems. It turned out, that for all highly active catalysts the coordination of the olefin is substantially lower in energy compared to less active systems. We are currently investigating other systems to verify the predictive power of this criterion for the search of even more active polymerization catalysts.

4.1. Computational details

All calculations were performed with GAUSSIAN98 [55]. The density functional hybrid model Becke3LYP [56–59] was used together with the valence double-ζ basis set 6-31G(d). Selected structures were additionally optimized using the triple-ζ basis set 6-311+G(d,p). No symmetry or internal coordinate constraints were applied during optimizations. All reported intermediates were verified as true minima by the absence of negative eigenvalues in the vibrational frequency analysis. Transition-state structures (indicated by **TS**) were located using the Berny algorithm [60] until the Hessian matrix had only one imaginary eigenvalue. The identity of all transition states was confirmed by the presence of one negative eigenvalue in the frequency analysis and animating this eigenvector coordinate with MOLDEN [61]. Approximate free energies were obtained through thermochemical analysis of the frequency calculation, using the thermal correction to the Gibbs free energy as reported by GAUSSIAN98. This takes into account zero-point effects, thermal enthalpy corrections, and entropy. All energies reported in this paper, unless otherwise noted, are free energies at 298 K and 1 atm. Frequencies remain unscaled. All transition states are maxima on the electronic potential energy surface. These may not correspond to maxima on the free energy surface. We did not attempt to correct the free energy for hindered internal rotations.

Kinetic isotope effects were calculated from free energy differences obtained from frequency calculations:

$$KIE = \frac{k_H}{k_D} = e^{\frac{\Delta G_D - \Delta G_H}{RT}} \tag{1}$$

$$\Delta G_X = G_X^{\neq} - G_X^{Educts} \quad X = H \text{ or } D \tag{2}$$

References

[1] L. Melander, W.H. Saunders, Reaction Rates of Isotopic Molecules, Wiley, New York, 1980.
[2] W.D. Jones, Acc. Chem. Res. 36 (2003) 140.
[3] H. Krauledat, H.H. Brintzinger, Angew. Chem. 102 (1990) 1459.
[4] W.E. Piers, J.E. Bercaw, J. Am. Chem. Soc. 112 (1990) 9406.
[5] M.K. Leclerc, H.H. Brintzinger, J. Am. Chem. Soc. 117 (1995) 1651.
[6] R.H. Grubbs, G.W. Coates, Acc. Chem. Res. 29 (1996) 85.
[7] J.A.N. Ajjou, S.L. Scott, J. Am. Chem. Soc. 122 (2000) 8968.
[8] M.H. Prosenc, C. Janiak, H.H. Brintzinger, Organometallics 11 (1992) 4036.
[9] A.K. Rappe, W.M. Skiff, C.J. Casewit, Chem. Rev. 100 (2000) 1435.
[10] R. Schmid, in: B. Cornils, W.A. Herrmann (Eds.), Applied Homogeneous Catalysis with Organometallic Compounds, Wiley-VCH, Weinheim, 2002, p. 712.
[11] G. Lanza, I.L. Fragala, T.J. Marks, Organometallics 21 (2002) 5594, and references therein.
[12] T. Yoshida, N. Koga, K. Morokuma, Organometallics 14 (1995) 746.
[13] T.K. Woo, P.M. Margl, J.C.W. Lohrenz, P.E. Bloechl, T. Ziegler, J. Am. Chem. Soc. 118 (1996) 13021.
[14] V.R. Jensen, W. Thiel, Organometallics 20 (2001) 4852.
[15] L. Resconi, L. Cavallo, A. Fait, F. Piemontesi, Chem. Rev. 100 (2000) 1253.
[16] W. Scherer, G.S. McGrady, Angew. Chem., Int. Ed. 43 (2004) 1782.
[17] S. Mecking, Angew. Chem., Int. Ed. 40 (2001) 534.
[18] V.C. Gibson, S.K. Spitzmesser, Chem. Rev. 103 (2003) 283.
[19] L. Deng, P. Margl, T. Ziegler, J. Am. Chem. Soc. 119 (1997) 1094.
[20] D.G. Musaev, R.D.J. Froese, K. Morokuma, Organometallics 17 (1998) 1850.
[21] T. Tomita, T. Takahama, M. Sugimoto, S. Sakaki, Organometallics 21 (2002) 4138.
[22] A. Michalak, T. Ziegler, Organometallics 18 (1999) 3998.
[23] L. Deng, P. Margl, T. Ziegler, J. Am. Chem. Soc. 121 (1999) 6479.
[24] D.V. Khoroshun, D.G. Musaev, T. Vreven, K. Morokuma, Organometallics 20 (2001) 2007.
[25] E. Kogut, A. Zeller, T.H. Warren, T. Strassner, J. Am. Chem. Soc. 126 (2004) 11984.
[26] M.J. Tanner, M. Brookhart, J.M. DeSimone, J. Am. Chem. Soc. 119 (1997) 7617.
[27] A. Zeller, T. Strassner, Organometallics 21 (2002) 4950.
[28] C. Wang, S. Friedrich, T.R. Younkin, R.T. Li, R.H. Grubbs, D.A. Bansleben, M.W. Day, Organometallics 17 (1998) 3149.
[29] T.R. Younkin, E.F. Connor, J.I. Henderson, S.K. Friedrich, R.H. Grubbs, D.A. Bansleben, Science 287 (2000) 460.
[30] F.A. Hicks, M. Brookhart, Organometallics 20 (2001) 3217.
[31] J.C. Jenkins, M. Brookhart, Organometallics 22 (2003) 250.
[32] F.A. Hicks, J.C. Jenkins, M. Brookhart, Organometallics 22 (2003) 3533.
[33] A. Michalak, T. Ziegler, Organometallics 22 (2003) 2069.
[34] M.S.W. Chan, L. Deng, T. Ziegler, Organometallics 19 (2000) 2741.
[35] D.V. Deubel, T. Ziegler, Organometallics 21 (2002) 1603.
[36] D.V. Deubel, T. Ziegler, Organometallics 21 (2002) 4432.
[37] S. Bhaduri, S. Mukhopadhyay, S.A. Kulkarni, J. Organomet. Chem. 654 (2002) 132.
[38] A. Michalak, T. Ziegler, Organometallics 20 (2001) 1521.
[39] Y. Liu, M. Zhang, M.G.B. Drew, Z.-D. Yang, Y. Liu, Theochem 726 (2005) 277.
[40] P. Cossee, Tetrahedron Lett. (1960) 12.

[41] P. Cossee, J. Catal. 3 (1964) 80.

[42] E.J. Arlman, P. Cossee, J. Catal. 3 (1964) 99.

[43] J.C. Jenkins, M. Brookhart, J. Am. Chem. Soc. 126 (2004) 5827.

[44] Calculations of important intermediates at the 6-311+G(d,p) level of theory showed only minor differences, e.g. $\Delta\Delta G$ between 3_O^{TS} and 3_N^{TS} then amounts to 7.6 kcal/mol. The insertion barrier, i.e. 2_O to 3_N^{TS}, is slightly lower with 14.3 kcal/mol, whereas the corresponding KIE remains almost constant ($k_H/k_D = 1.10$).

[45] D.G. Musaev, R.D.J. Froese, M. Svensson, K. Morokuma, J. Am. Chem. Soc. 119 (1997) 367.

[46] At higher pressures the alkyl ethylene complex becomes more favorable. Accordingly, our calculations revealed that 2_O is 2.4 (at 20 bar) or 2.6 kcal/mol (at 50 bar) lower in energy relative to 1_O.

[47] D.A. Singleton, A.A. Thomas, J. Am. Chem. Soc. 117 (1995) 9357.

[48] D.E. Frantz, D.A. Singleton, J.P. Snyder, J. Am. Chem. Soc. 119 (1997) 3383.

[49] A.J. DelMonte, J. Haller, K.N. Houk, K.B. Sharpless, D.A. Singleton, T. Strassner, A.A. Thomas, J. Am. Chem. Soc. 119 (1997) 9907.

[50] C.R. Landis, K.A. Rosaaen, J. Uddin, J. Am. Chem. Soc. 124 (2002) 12062.

[51] S. Juengling, R. Muelhaupt, U. Stehling, H.H. Brintzinger, D. Fischer, F. Langhauser, J. Polym. Sci., Part A: Polym. Chem. 33 (1995) 1305.

[52] L.K. Johnson, C.M. Killian, M. Brookhart, J. Am. Chem. Soc. 117 (1995) 6414.

[53] S.D. Ittel, L.K. Johnson, M. Brookhart, Chem. Rev. 100 (2000) 1169.

[54] N.A. Cooley, S.M. Green, D.F. Wass, K. Heslop, A.G. Orpen, P.G. Pringle, Organometallics 20 (2001) 4769.

[55] M.J. Frisch, G.W. Trucks, H.B. Schlegel, G.E. Scuseria, M.A. Robb, J.R. Cheeseman, V.G. Zakrzewski, J.A. Montgomery, R.E. Stratmann, J.C. Burant, S. Dapprich, J.M. Millam, A.D. Daniels, K.N. Kudin, M.C. Strain, O. Farkas, J. Tomasi, V. Barone, M. Cossi, R. Cammi, B. Mennucci, C. Pomelli, C. Adamo, S. Clifford, J. Ochterski, G.A. Petersson, P.Y. Ayala, Q. Cui, K. Morokuma, D.K. Malick, A.D. Rabuck, K. Raghavachari, J.B. Foresman, J. Cioslowski, J.V. Ortiz, A.G. Baboul, B.B. Stefanov, G. Liu, A. Liashenko, P. Piskorz, I. Komaromi, R. Gomperts, R.L. Martin, D.J. Fox, T. Keith, M.A. Al-Laham, C.Y. Peng, A. Nanayakkara, C. Gonzalez, M. Challacombe, P.M.W. Gill, B. Johnson, W. Chen, M.W. Wong, J.L. Andres, C. Gonzalez, M. Head-Gordon, E.S. Replogle, J.A. Pople, GAUSSIAN 98, Revision A.7, Gaussian, Inc., Pittsburgh, PA, 1998.

[56] C. Lee, W. Yang, R.G. Parr, Phys. Rev. B: Condens. Matter 37 (1988) 785.

[57] S.H. Vosko, L. Wilk, M. Nusair, Can. J. Phys. 58 (1980) 1200.

[58] P.J. Stephens, F.J. Devlin, C.F. Chabalowski, M.J. Frisch, J. Phys. Chem. 98 (1994) 11623.

[59] A.D. Becke, J. Chem. Phys. 98 (1993) 5648.

[60] C. Peng, P. Ayala, H.B. Schlegel, M.J. Frisch, J. Comput. Chem. 17 (1996) 49.

[61] G. Schaftenaar, J.H. Noordik, J. Comput. Aided Mol. Des. 14 (2000) 123.

[62] T.K. Woo, P.E. Bloechl, T. Ziegler, J. Phys. Chem. A 104 (2000) 121.